J. Plasma Physics (2011), *vol.* 77, *part* 4, *pp.* 537–545. © Cambridge University Press 2010
doi:10.1017/S0022377810000711

Turbulence changes from magnetic fields in a stationary plasma

A. B. ALEXANDER, C. T. RAYNOR, D. L. WIGGINS, M. K. ROBINSON, C. C. AKPOVO and J. A. JOHNSON III

Center for Plasma Science and Technology, Florida A&M University, Tallahassee, FL 32310, USA
(abalexander@cepast.famu.edu)

(Received 1 November 2010; accepted 29 November 2010; first published online 23 December 2010)

Abstract. When the krypton plasma in a DC glow discharge tube is exposed to an axial magnetic field, the turbulent energy and the characteristic dominant mode in the turbulent fluctuations are systematically and unexpectedly reduced with increasing magnetic field strength. When the index measuring the rate of transfer of energy through fluctuation scales is monitored, a lambda-like dependence on turbulent energy is routinely observed in all magnetic fields. From this, a critical turbulent energy is identified, which also decreases with increasing magnetic field strength.

1. Introduction

Turbulence in magnetically confined toroidal plasmas has a long history and relevance due to the detrimental role of turbulence-induced transport on particle, energy, impurity and momentum confinement [1]. In fact, the reorganization of plasmas because of turbulence is among the most important processes that occur in both planetary magnetospheres as well as fusion energy research [2]. It is well known that turbulent fluctuations in glow discharge plasmas have pronounced dimensionality [3]. Although it has already been shown that plasmas in a DC glow discharge can be turbulent [4], there have been no studies to determine if the turbulence in these discharges with their built-in dimensionality magnetic field lever can be manipulated. Specifically by focusing on magnetic fields, such studies might be of particular benefit to those interested in the possibility of control of the characteristics of a turbulent system in magnetized turbulent fusion plasmas and the collateral control of astrophysical plasmas that may come from nearby magnetic fields. We have already seen that a weak magnetic field can have profound effects on the turbulence behind ionizing shock waves [5]. Therefore, we begin our investigations of the role that a weak magnetic field might play in modifying the turbulence in glow discharge plasmas. We first look at some of the general characteristics of the plasma, such as electron density and temperature. Then we compute the characteristic frequency, spectral index and the turbulent energy. We treat the change from non-turbulent to turbulent in both the un-magnetized and magnetized DC glow discharge. Finally, we investigate the influence of a magnetic field on the critical turbulent energy.

https://doi.org/10.1017/S0022377810000711 Published online by Cambridge University Press

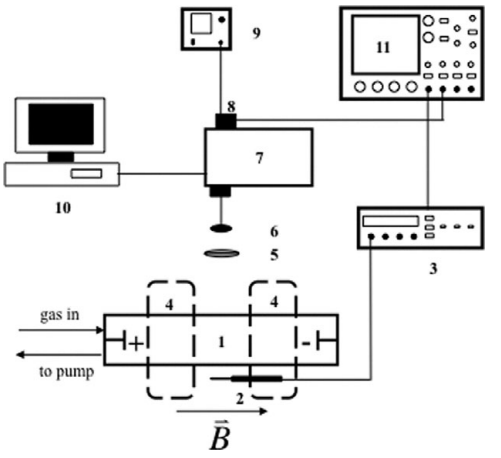


Figure 1. A schematic diagram of the glow discharge plasma apparatus.

2. Experimental setup

The experimental setup is shown in Fig. 1. It includes the following items: (1) quartz discharge tube, (2) gaussmeter probe, (3) gaussmeter, (4) Helmholtz coils, (5) 30-cm focal length bi-convex lens, (6) fiber optic cable & cable mount, (7) monochromator with a mounted wide band pass spectrograph, (8) photomultiplier tube (PMT), (9) PMT power supply, (10) computer and (11) Tektronix DPO 7000 series oscilloscope.

The circuit used to operate the glow discharge is simple. It consists of a DC power supply, a resistor and a quartz tube. The power supply is capable of operating at 10 kV and 2 A through 10-kW load resistor. The quartz tube is 53-cm long and has a 2.5-cm diameter. The quart tube is first evacuated using a pumping system, connected through a series of O-ring joints. The pumping system consists of a dry pump with a top speed of 3.7 L s^{-1} and a turbo molecular pump with a speed of 220 L s^{-1}; collectively the system is pumped to a base pressure of roughly 10^{-6} Torr, and is pressurized with an ultra-high purity (99.99%) krypton gas to 500 m Torr. The vacuum pressure in monitored by a Varian active ion gauge, while the Baratron capacitance manometer indicates the absolute gas pressure during data collection. The DC power supply is set at 40 mA and 450 V. The current flowing through the krypton gas generates the stationary glow discharge plasma between the two electrodes in the tube. The cathode consists of a tungsten grid, 2 cm in diameter. Light emitted from the plasma in the discharge tube is then collected optically using a simple bi-convex lens. A typical area of analysis is 2×2 cm, with a height of 5 cm, perpendicular to the discharge axis. The lens then focuses the light onto a fiber optic cable with a 1-mm diameter. The light from the fiber optic cable then enters the entrance slit of a 0.5-m focal length monochromator, yielding a spectral resolution of 0.1 nm.

Using the monochromator software installed on the computer, the monochromator is set to permit light from the range of lines 700 to 830 nm to travel through it and strike the PMT. The signal of the detected light is then amplified and displayed on the oscilloscope as changes in voltage. The light signal is captured at a rate of 250 kilo-samples per second for 250 ms.

https://doi.org/10.1017/S0022377810000711 Published online by Cambridge University Press

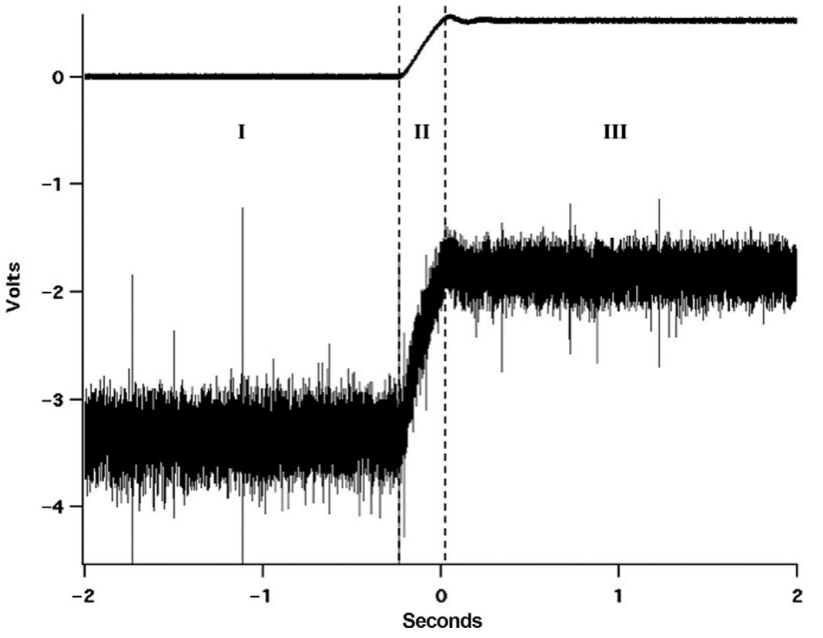


Figure 2. Oscilloscope displays of voltages corresponding to the magnetic field and emission intensities as a function of time. The thin upper line refers to the magnetic field. The lower signal represents the plasma emission.

The uniform magnetic field generated by the Helmholtz coils points in a direction parallel to the direction of the current flow, and can be varied from 0–500 Gauss. It is measured using a gaussmeter and gaussmeter probe. The gaussmeter reading is then converted to a change in voltage and displayed on the oscilloscope.

3. Analytical techniques

Generally speaking, there is no theoretical or experimental motivation to expect a routine role for an axial magnetic field, as distinguished from fields in planetary magnetospheres [6], on turbulent fluctuations in a stationary plasma. Nonetheless, we have observed that standard glow discharges are typically more stable (less noisy) under the influence of an applied steady axial magnetic field. Figure 2 shows the time-evolved behavior of the glow discharge plasma in a krypton gas driven by a magnetic field, as well as the evolution of the magnetic field itself.

It takes roughly 250 ms for the magnetic field to rise from zero to predetermined magnetic field level (i.e. 150 Gauss, 300 Gauss). During this time it is clear that the magnetic field has a noticeable effect on the fluctuations. We notice that the voltage readings for the magnetic field and light fluctuations increase after the magnetic field is turned on. Both signal profiles follow one another during the rise of the magnetic field till it stabilizes. During the magnetic field stabilization, we notice that the thickness of the light fluctuation's voltage signal decreases.

Next, we collect light fluctuations under the influence of a steady magnetic field. The magnetic field range was from zero to 500 Gauss in 50 Gauss increments. For each magnetic field, we collected 10 sets of runs, each of 50 000 points in record

https://doi.org/10.1017/S0022377810000711 Published online by Cambridge University Press

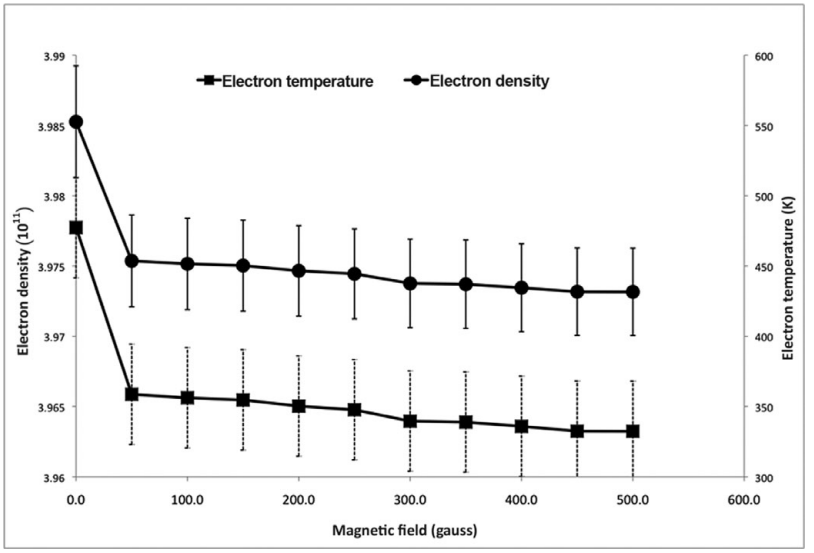


Figure 3. Electron temperature (T_e) and density (n_e) plotted versus magnetic field. Error bars represent $\pm 7\%$ and $\pm 11\%$ for T_e and n_e, respectively.

length. At the same time we used a CCD attached to a wide band pass spectrograph to collect spectral readings of four neutral lines to be used to determine electron temperature and density and plasma frequency.

Finally, we look at the turbulent parameters of the krypton plasma under the influence of a steady magnetic field. The characteristic frequency is the strongest frequency in the Fourier transform of the power spectrum. It is easily identified as the position of the highest peak of the power spectrum. The spectral index measures the scale dependence of the size of perturbations in the plasma. These perturbations are described by a power spectrum, which measures their amplitude as a function of wavelength. In particular, if the perturbations are assumed to have a power-law form in wave number $P_k \propto f_k^{-n}$, then the spectral index is the power n that appears. In this case, it is an indicator of how the turbulent kinetic energy fluctuations move from large to small scales. The turbulent energy is taken by integrating the power spectrum using $E_\tau = \sum_{i=o}^{\text{noise}} (P_k)_i$. As an aid to interpreting these data, we apply the Ginzburg–Landau second-order phase transformation to the interpretation of transition to turbulence. Using this inherently thermodynamical approach, we can expect to see a lambda (λ)-like evolution of the turbulent parameters when plotted against turbulent energy.

4. Results and discussion

The relatively low temperatures of the plasma make any thermal effects that might cause confusing consequences for our turbulent studies below unlikely. Figure 3 shows specifically that (using the intensity-ratio method [7] for each run) when the magnetic field is of zero Gauss, there is little fluctuation in the electron density.

When the relative line intensity method is used to determine the Stark-broadening characteristics, the Boltzmann function can be used to calculate the electron

https://doi.org/10.1017/S0022377810000711 Published online by Cambridge University Press

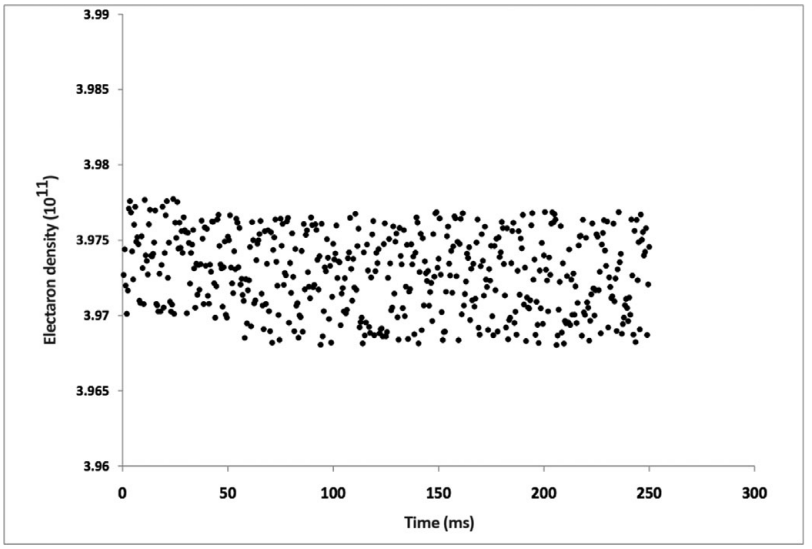


Figure 4. Electron density (n_e) versus time for multiple sets of 10 runs. No magnetic field was applied to the plasma while these data were obtained.

temperature [8] and density [9]. The results of these determinations for a complete set of our magnetic fields are shown in Fig. 4. It's clear that around 50 Gauss the magnetic field greatly reduces both the electron temperature and density of the krypton plasma.

We begin our turbulence analysis by performing a Fourier transformation on the turbulent fluctuation data of each of the 10 runs. As stated previously, the data are collected under steady state magnetic field conditions. We obtain the characteristic frequency, turbulent energy, spectral index and chaotic dimension, following the turbulent analysis methods outlined recently [5].

A representative set of plots of power spectra for determination of the characteristic frequency is shown in Fig. 5 for three different magnetic field strengths. The characteristic frequency is shown for all measured field strengths in Fig. 6. This plot also shows, after 150 Gauss, a systematic decrease in the characteristic frequency with increasing magnetic field strength.

The evolution of turbulent energy with time is shown in Fig. 7. Here we see that during the ramp up of the magnetic field, stages II and III as defined in Fig. 2, the turbulent energy is suppressed by a weak magnetic field. The strength of the turbulent light fluctuations has been substantially suppressed by 50–70%.

Figure 8 shows a representative log power versus log frequency plot from which we obtain the spectral index. Specifically, the value of the spectral index is determined by taking the slope of power spectrum in the indicated Kolmogorov region, defined as the frequencies after the power input region but before the high frequency signals, which precede the noise. Using turbulent energies as defined earlier, we show in Fig. 9 samples of plots of the spectral index versus the turbulent energy for zero Gauss and 300 Gauss. For this, the spectral index takes on the role of a transport parameter. When the result is compared to the standard profile of the Ginzburg–Landau second-order phase transition [10], the approximate λ-like profile is clearly

https://doi.org/10.1017/S0022377810000711 Published online by Cambridge University Press

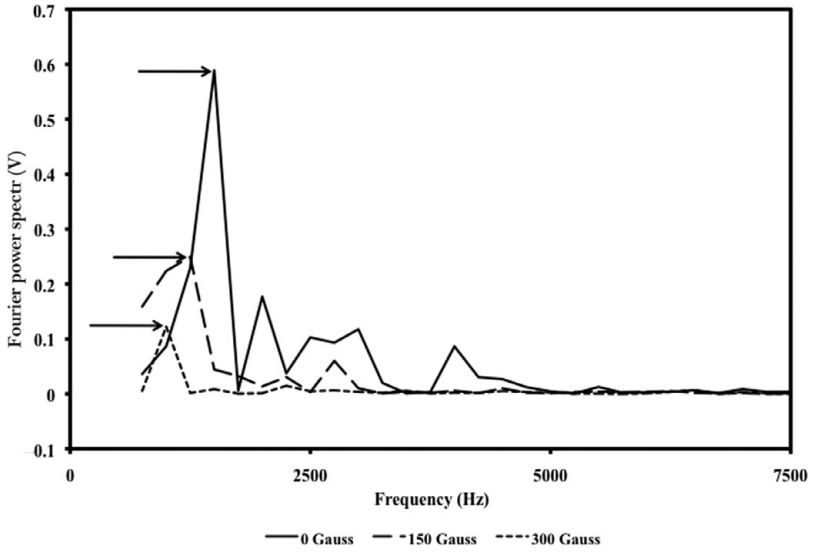


Figure 5. Sample frequency spectrum from the power spectrum for zero, 150 and 300 Gauss. The characteristic frequency is indicated by the strongest signal in the spectrum.

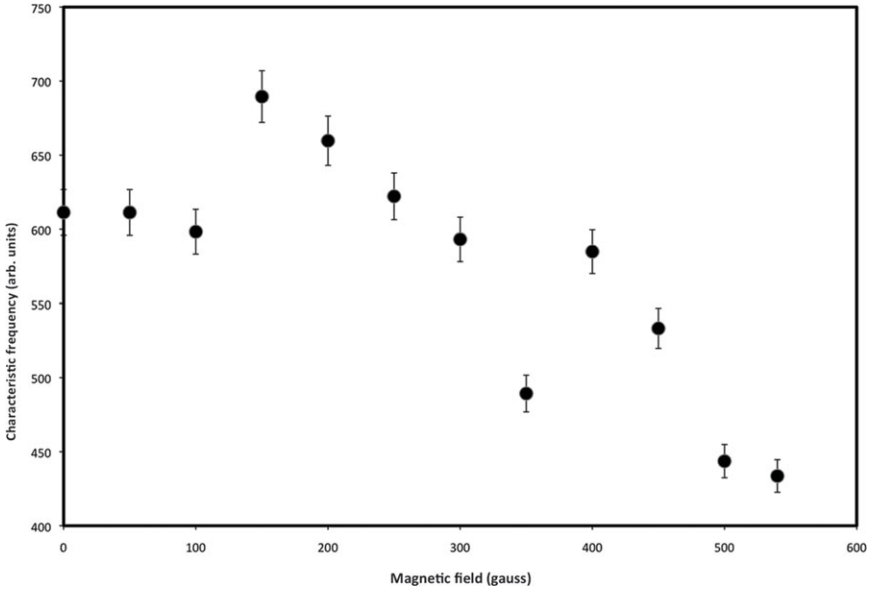


Figure 6. Magnetic field versus characteristic frequency is shown. The characteristic frequency steadily decreases with an increase in magnetic field strength. Error bars for characteristic frequency represent a standard deviation of $\pm 2.5\%$.

visible. The arrows in Fig. 9 indicate the location and thus the value of the critical turbulent energy.

Using similar approximate λ-like profiles for other magnetic field strengths, we identify critical turbulent energies for our glow discharge plasma. The results of these determinations are shown in Fig. 10. Here we can clearly see a trend suggesting that an increasing magnetic field reduces the critical turbulent energy.

https://doi.org/10.1017/S0022377810000711 Published online by Cambridge University Press

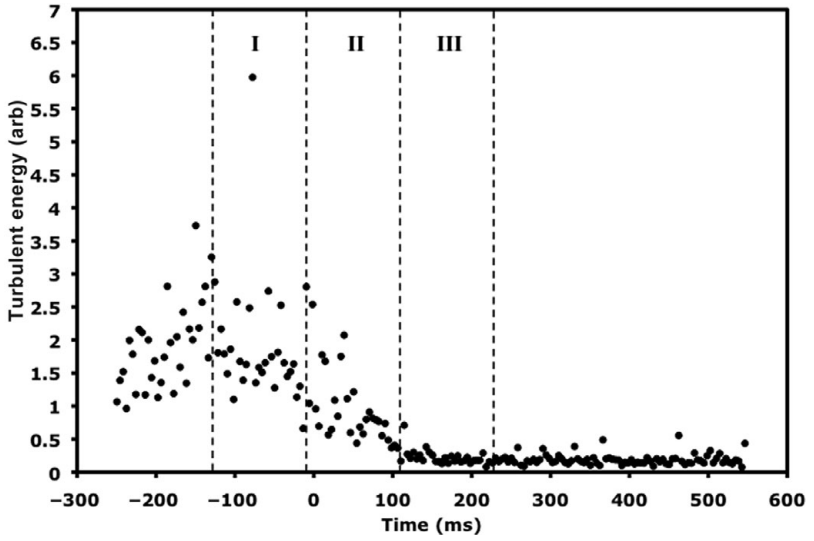


Figure 7. The time evolution of turbulent energy showing three regions of analysis. The turbulent energy is given by the integration of a power spectrum, such as Fig. 6.

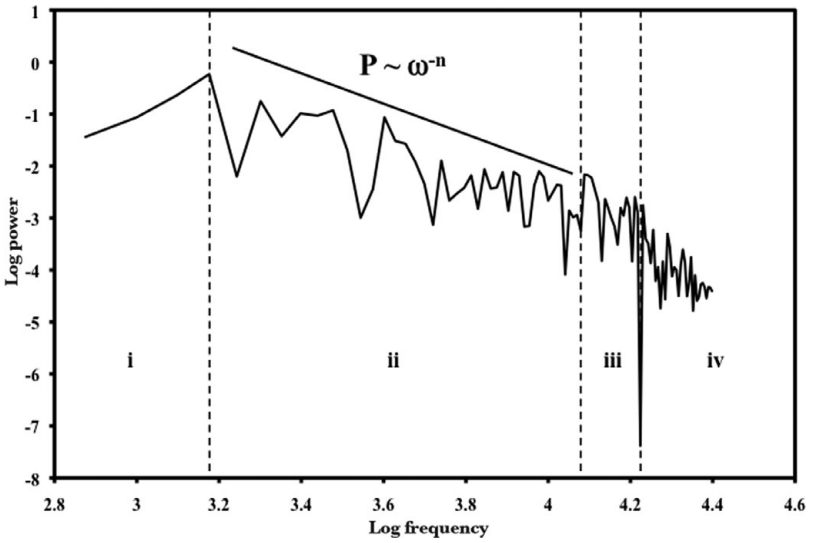


Figure 8. Sample log power versus log frequency for a typical power spectrum. The Kolmogorov region is indicated for the determination of spectral index.

5. Conclusion

Evidence has been found suggesting that a weak magnetic field can indeed depress the turbulent energy in the glow discharge tube as well as the characteristic dominant frequency. Because of the observation of a λ-like behavior in the dependence of a transport parameter on local energy, one can interpret the turbulent fluctuation data in a glow discharge tube as showing behavior consistent with the use of a

https://doi.org/10.1017/S0022377810000711 Published online by Cambridge University Press

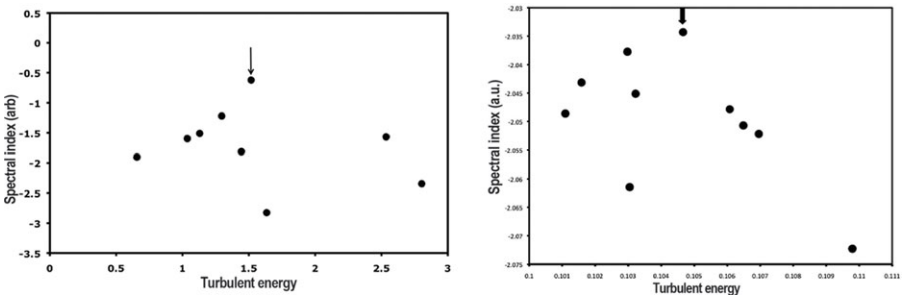


Figure 9. Sample critical turbulent energies for (a) 0 Gauss and (b) 300 Gauss calculated from a plot of the spectral index versus turbulent energy at zero Gauss. The phase transition point, defined by an approximate λ-like profile, is indicated.

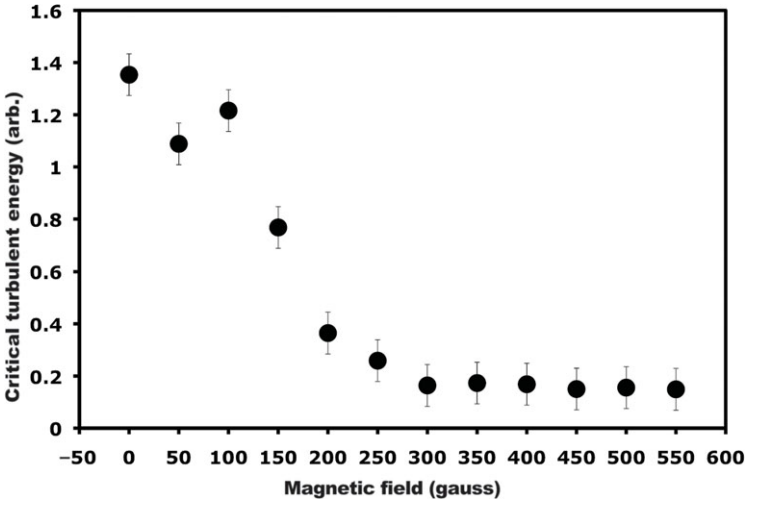


Figure 10. Sample critical turbulent energy plot versus the evolving magnetic field. The decaying nature of the turbulent energy implies sensitivity to the relative strength of the magnetic field. Error bars for turbulent energy represent a standard deviation of $\pm 3.2\%$.

second-order phase transformation approach in these analyses. From this approach, evidence has also been found of a dependency of critical turbulent energy in these krypton plasmas on magnetic field strength quite similar to evidence previously reported for magnetized turbulent argon plasmas behind ionizing shock waves [5].

Acknowledgments

This research was supported in part by funding from the National Science Foundation to Florida A&M University.

References

[1] Conway, G. D. 2008 Turbulence measurements in fusion plasmas. *Plasma Phys. Control. Fusion* **50**(12), 124026.

https://doi.org/10.1017/S0022377810000711 Published online by Cambridge University Press

[2] Boxer, A. C., Bergmann, R., Ellsworth, J. L., Garnier, D. T., Kesner, J., Mauel, M. E. et al. 2010 Turbulent inward pinch of plasma confined by a levitated dipole magnet. *Nat. Phys.* **6**(3), 207–212 [10.1038/nphys1510].

[3] Johnson III, J. A. and Ramaiah, R. 1987 Plasma instability in the presence of negative ions. *Phys. Rev.* A **36**(2), 774.

[4] Johnson III, J. A., Johnson, L. E. and Hong, Y. 1991 Dimensional analysis in a turbulent glow discharge plasma. *Phys. Lett.* A **158**(3–4), 144–148.

[5] Raynor, C. T., Mezonlin, E. D. and Johnson III, J. A. 2009 Critical turbulent energy reductions in plasmas using weak magnetic fields. *J. Appl. Phys.* **105**(4), 043301–043306.

[6] Retino, A., Sundkvist, D., Valvads, A., Mozer, F., Andre, M. and Owen, C. J. 2007 In situ evidence of magnetic reconnection in turbulent plasma. *Nat. Phys.* **3**(4), 236–238 [10.1038/nphys574].

[7] Podder, N. K., Johnson III, J. A., Raynor, C. T., Loch, S. D., Ballance, C. P. and Pindzola, M. S. 2004 Helium line intensity ratio in microwave-generated plasmas. *Phys. Plasmas* **11**(12), 5436–5443.

[8] Namihira, T., Sakai, S., Yamaguchi, T., Yamamoto, K., Yamada, C., Kiyan, T. et al. 2007 Electron temperature and electron density of underwater pulsed discharge plasma produced by solid-state pulsed-power generator. *Plasma Sci. IEEE Trans.* **35**(3), 614–618.

[9] Milosavljevic, V., Djenize, S. and Dimitrijevic, M. S. 2003 Experimental and calculated stark widths within the Kr I spectrum. *Phys. Rev.* E **68**(1), 016402.

[10] Landau, L. D. and Lifshitz, E. M. 1987 *Fluid Mechanics*. Oxford, UK: Reed Educational and Professional.

https://doi.org/10.1017/S0022377810000711 Published online by Cambridge University Press